AMERICAN SOCIETY FOR MICROBIOLOGY | Journal of Virology®

VIRUS-CELL INTERACTIONS

Molecular Mechanism for Antibody-Dependent Enhancement of Coronavirus Entry

Yushun Wan,[a] Jian Shang,[a] Shihui Sun,[b] Wanbo Tai,[c] Jing Chen,[d] Qibin Geng,[a] Lei He,[b] Yuehong Chen,[b] Jianming Wu,[a] Zhengli Shi,[d] Yusen Zhou,[b] Lanying Du,[c] Fang Li[a]

[a]Department of Veterinary and Biomedical Sciences, College of Veterinary Medicine, University of Minnesota, Saint Paul, Minnesota, USA
[b]Laboratory of Infection and Immunity, Beijing Institute of Microbiology and Epidemiology, Beijing, China
[c]Lindsley F. Kimball Research Institute, New York Blood Center, New York, New York, USA
[d]Wuhan Institute of Virology, Chinese Academy of Sciences, Wuhan, Hubei Province, China

Yushun Wan and Jian Shang contributed equally to this work. Author order was determined by the time of joining the project.

ABSTRACT Antibody-dependent enhancement (ADE) of viral entry has been a major concern for epidemiology, vaccine development, and antibody-based drug therapy. However, the molecular mechanism behind ADE is still elusive. Coronavirus spike protein mediates viral entry into cells by first binding to a receptor on the host cell surface and then fusing viral and host membranes. In this study, we investigated how a neutralizing monoclonal antibody (MAb), which targets the receptor-binding domain (RBD) of Middle East respiratory syndrome (MERS) coronavirus spike, mediates viral entry using pseudovirus entry and biochemical assays. Our results showed that MAb binds to the virus surface spike, allowing it to undergo conformational changes and become prone to proteolytic activation. Meanwhile, MAb binds to cell surface IgG Fc receptor, guiding viral entry through canonical viral-receptor-dependent pathways. Our data suggest that the antibody/Fc-receptor complex functionally mimics viral receptor in mediating viral entry. Moreover, we characterized MAb dosages in viral-receptor-dependent, Fc-receptor-dependent, and both-receptors-dependent viral entry pathways, delineating guidelines on MAb usages in treating viral infections. Our study reveals a novel molecular mechanism for antibody-enhanced viral entry and can guide future vaccination and antiviral strategies.

IMPORTANCE Antibody-dependent enhancement (ADE) of viral entry has been observed for many viruses. It was shown that antibodies target one serotype of viruses but only subneutralize another, leading to ADE of the latter viruses. Here we identify a novel mechanism for ADE: a neutralizing antibody binds to the surface spike protein of coronaviruses like a viral receptor, triggers a conformational change of the spike, and mediates viral entry into IgG Fc receptor-expressing cells through canonical viral-receptor-dependent pathways. We further evaluated how antibody dosages impacted viral entry into cells expressing viral receptor, Fc receptor, or both receptors. This study reveals complex roles of antibodies in viral entry and can guide future vaccine design and antibody-based drug therapy.

KEYWORDS antibody-dependent enhancement of viral entry, MERS coronavirus, SARS coronavirus, spike protein, neutralizing antibody, viral receptor, IgG Fc receptor, antibody-dependent enhancement of viral entry

Antibody-dependent enhancement (ADE) occurs when antibodies facilitate viral entry into host cells and enhance viral infection in these cells (1, 2). ADE has been observed for a variety of viruses, most notably flaviviruses (e.g., dengue virus) (3–6). It has been shown that when patients are infected by one serotype of dengue virus (i.e.,

Citation Wan Y, Shang J, Sun S, Tai W, Chen J, Geng Q, He L, Chen Y, Wu J, Shi Z, Zhou Y, Du L, Li F. 2020. Molecular mechanism for antibody-dependent enhancement of coronavirus entry. J Virol 94:e02015-19. https://doi.org/10.1128/JVI.02015-19.

Editor Tom Gallagher, Loyola University Chicago

Address correspondence to Lanying Du, LDu@nybc.org, or Fang Li, lifang@umn.edu.

Received 27 November 2019
Accepted 4 December 2019
Accepted manuscript posted online 11 December 2019
Published 14 February 2020

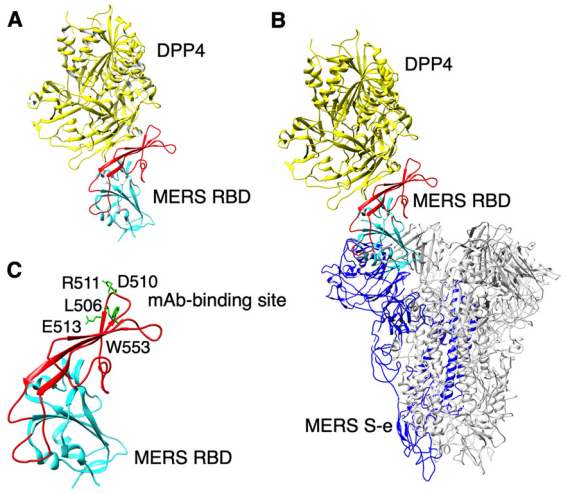

FIG 1 Structural similarity between DPP4 and MAb in binding MERS-CoV spike. (A) Tertiary structure of MERS-CoV RBD in complex with DPP4 (PDB code 4KR0) (30). DPP4 is colored yellow. RBD is colored cyan (core structure) and red (receptor-binding motif). DPP4 binds to the receptor-binding motif of the RBD. (B) Modeled structure of MERS-CoV S-e in complex with DPP4. S-e is a trimer (PDB code 5X5F): one monomeric subunit, whose RBD is in the standing-up conformation, is colored blue, and the other two monomeric subunits, whose RBDs are in the lying-down conformation, are colored gray (18). To generate the structural model of the S-e in complex with DPP4, the RBD in panel A was structurally aligned with the standing-up RBD in the S-e trimer. (C) Tertiary structure of MERS-CoV RBD (PDB code 4L3N) (64). Critical MAb-binding residues were identified through mutagenesis studies (48) and are shown as green sticks.

primary infection), they produce neutralizing antibodies targeting the same serotype of the virus. However, if they are later infected by another serotype of dengue virus (i.e., secondary infection), the preexisting antibodies cannot fully neutralize the virus. Instead, the antibodies first bind to the virus and then bind to the IgG Fc receptors on immune cells and mediate viral entry into these cells. A similar mechanism has been observed for HIV and Ebola viruses (7–10). Thus, subneutralizing antibodies (or non-neutralizing antibodies in some cases) are responsible for ADE of these viruses. Given the critical roles of antibodies in host immunity, ADE causes serious concerns in epidemiology, vaccine design, and antibody-based drug therapy. This study reveals a novel mechanism for ADE in which fully neutralizing antibodies mimic the function of viral receptor in mediating viral entry into Fc receptor-expressing cells.

Coronaviruses are a family of large, positive-stranded, and enveloped RNA viruses (11, 12). Two highly pathogenic coronaviruses, severe acute respiratory syndrome coronavirus (SARS-CoV) and Middle East respiratory syndrome coronavirus (MERS-CoV), cause lethal infections in humans (13–16). An envelope-anchored spike protein guides coronavirus entry into host cells (17). As a homotrimer, the spike contains three receptor-binding S1 subunits and a trimeric membrane fusion S2 stalk (18–25). This state of the spike on the mature virions is called "prefusion." SARS-CoV and MERS-CoV recognize angiotensin-converting enzyme 2 (ACE2) and dipeptidyl peptidase 4 (DPP4), respectively, as their viral receptors (26–28). Their S1 subunits each contain a receptor-binding domain (RBD) that mediates receptor recognition (29, 30) (Fig. 1A). The RBD is located on the tip of the spike trimer and is present in two different states: standing up and lying down (18, 21) (Fig. 1B). Binding to a viral receptor can stabilize the RBD in the standing-up state (20). Receptor binding also triggers the spike to undergo further conformational changes, allowing host proteases to cleave at two sites sequentially: first at the S1/S2 boundary (i.e., S1/S2 site) and then within S2 (i.e., S2′ site) (31, 32). Proteolysis of the spike can take place during viral maturation (by proprotein convertases), after viral release (by extracellular proteases), after viral attachment (by cell surface proteases), or after viral endocytosis (by lysosomal proteases) (33–39). After two protease cleavages, S1 dissociates and S2 undergoes a dramatic structural change to

fuse host and viral membranes; this membrane fusion state of the spike is called "postfusion" (40, 41). Due to the recent progress toward understanding the receptor recognition and membrane fusion mechanisms of coronavirus spikes, coronaviruses represent an excellent model system for investigating ADE of viral entry.

ADE has been observed for coronaviruses. Several studies have shown that sera induced by SARS-CoV spike enhance viral entry into Fc receptor-expressing cells (42–44). Further, one study demonstrated that unlike receptor-dependent viral entry, serum-dependent SARS-CoV entry does not go through the endosome pathway (44). Additionally, it has long been known that immunization of cats with feline coronavirus spike leads to worsened future infection due to the induction of infection-enhancing antibodies (45–47). However, detailed molecular mechanisms for ADE of coronavirus entry are still unknown. We previously discovered a monoclonal antibody (MAb) (named Mersmab1) which has strong binding affinity for MERS-CoV RBD and efficiently neutralizes MERS-CoV entry by outcompeting DPP4 (48); this discovery allowed us to comparatively study the molecular mechanisms for antibody-dependent and receptor-dependent viral entries.

In this study, we examined how Mersmab1 binds to MERS-CoV spike, triggers the spike to undergo conformational changes, and mediates viral entry into Fc receptor-expressing cells. We also investigated the pathways and antibody dosages for Mersmab1-dependent and DPP4-dependent viral entries. Our study sheds lights on the mechanisms of ADE and provides insight into vaccine design and antibody-based antiviral drug therapy.

RESULTS

Antibody-dependent enhancement of coronavirus entry. To investigate ADE of coronavirus entry, we first characterized the interactions between Mersmab1 (which is a MERS-CoV RBD-specific MAb) and MERS-CoV spike using biochemical methods. First, enzyme-linked immunosorbent assay (ELISA) was performed between Mermab1 and MERS-CoV RBD and between Mersmab1 and MERS-CoV spike ectodomain (S-e) (Fig. 2A). To this end, Mersmab1 (which was in excess) was used to coat the ELISA plate, and gradient amounts of recombinant RBD or S-e were added for detection of potential binding to Mersmab1. The results showed that both the RBD and S-e bound to Mersmab1. S-e bound to Mersmab1 more tightly than the RBD did, likely due to the multivalent effects associated with the trimeric state of S-e. Second, we prepared Fab from Mersmab1 using papain digestion and examined the binding between Fab and S-e using ELISA. Recombinant S-e (which was in excess) was used to coat the ELISA plate, and gradient amounts of Fab or Mersmab1 were added for detection of potential binding to S-e. The results showed that both Fab and Mersmab1 bound to S-e (Fig. 2B). Mersmab1 bound to S-e more tightly than Fab did, also likely due to the multivalent effects associated with the dimeric state of Mersmab1. Third, a flow cytometry assay was carried out to detect the binding between S-e and the DPP4 receptor and among S-e, Mersmab1, and CD32A (which is an Fc receptor). To this end, DPP4 or CD32A was expressed on the surface of human HEK293T cells (human kidney cells), and recombinant S-e was added for detection of potential binding to one of the two receptors in the absence or presence of Mersmab1. The results showed that without Mersmab1, S-e bound to DPP4 only; in the presence of Mersmab1, S-e bound to CD32A (Fig. 2C). As a negative control, a SARS-CoV RBD-specific MAb (49) did not mediate the binding of S-e to CD32A. The cell surface expressions of both DPP4 and CD32A were measured and used for calibrating the flow cytometry result (Fig. 2D), demonstrating that the direct binding of S-e to DPP4 is stronger than the indirect binding of S-e to CD32A through Mersmab1. Overall, these biochemical results reveal that Mersmab1 not only directly binds to the RBD region of MERS-CoV S-e but also mediates the indirect binding interactions between MERS-CoV S-e and the Fc receptor.

Next, we investigated whether Mersmab1 mediates MERS-CoV entry into Fc receptor-expressing cells. To this end, we performed a MERS-CoV pseudovirus entry assay, in which retroviruses pseudotyped with MERS-CoV spike (i.e., MERS-CoV pseu-

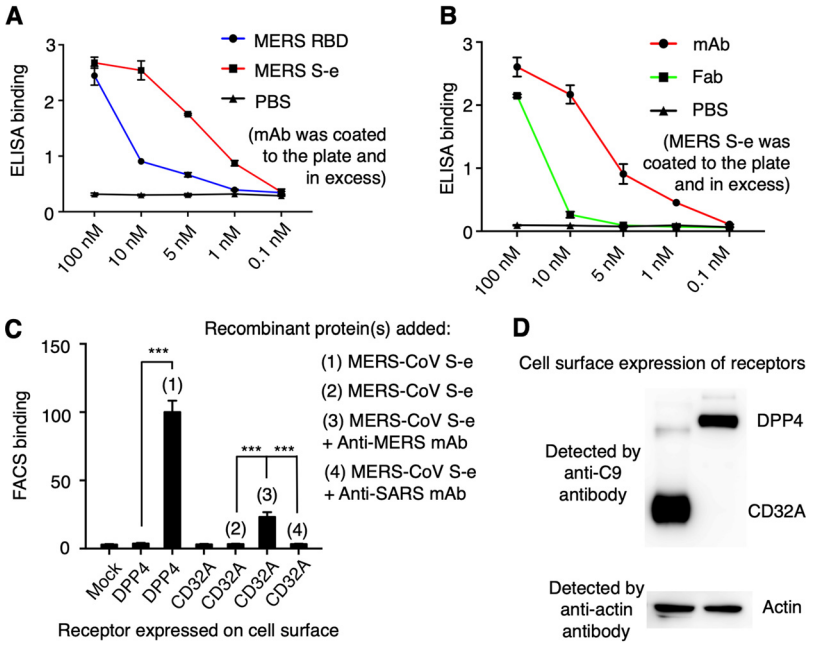

FIG 2 Interactions between coronavirus spike and RBD-specific MAb. (A) ELISA for detection of the binding between MERS-CoV RBD-specific MAb (i.e., Mersmab1) and MERS-CoV spike ectodomain (S-e). Mersmab1 was precoated on the plate, and recombinant S-e or RBD was added subsequently for ELISA. Binding affinities were characterized as ELISA signal at an optical density (OD) at 450 nm. PBS was used as a negative control. (B) ELISA for detection of the binding between Fab of Mersmab1 and MERS-CoV S-e. Recombinant S-e was used to precoat the plate, and Mersmab1 or Fab was added subsequently for ELISA. (C) Flow cytometry for detection of the binding between MERS-CoV S-e and DPP4 receptor and among S-e, Mersmab1, and CD32A (i.e., Fc receptor). Cells expressing DPP4 or CD32A were incubated with S-e alone, S-e plus Mersmab1, or S-e plus a SARS-CoV RBD-specific MAb (i.e., 33G4). Fluorescence-labeled anti-His_6 antibody was added to target the C-terminal His_6 tag on S-e. Cells were analyzed using fluorescence-activated cell sorting (FACS). (D) The expression levels of cell-membrane-associated DPP4 and CD32A were characterized using Western blotting targeting their C-terminal C9 tag and then used to normalize the binding affinity as measured in panel C. As an internal control, the expression level of cellular actin was measured using an anti-actin antibody. All of the experiments were repeated at least three times, with similar results, and representative results are shown. Error bars indicate SD ($n = 5$). Statistical analyses were performed as a one-tailed t test. ***, $P < 0.001$. Mersmab1 and its Fab both bind to MERS-CoV RBD and S-e.

doviruses) were used to enter human cells expressing CD32A on their surface. The main advantage of pseudovirus entry assay is to focus on the viral entry step (which is mediated by MERS-CoV spike) by separating viral entry from the other steps of viral infection cycles (e.g., replication, packaging, and release). We tested three different types of Fc receptors: CD16A, CD32A, and CD64A; each of these Fc receptors was exogenously expressed in HEK293T cells. We also tested macrophages in which mixtures of Fc receptors were endogenously expressed. The absence of Mersmab1 served as a control for Mersmab1 (a nonneutralizing MAb would be appropriate as another control for Mersmab1, but we do not have access to any nonneutralizing MAb). The results showed that in the absence of Mersmab1, MERS-CoV pseudoviruses could not enter Fc receptor-expressing cells; in the presence of Mersmab1, MERS-CoV pseudoviruses demonstrated significant efficiency in entering CD32A-expressing HEK293T cells and macrophages (Fig. 3A). In comparison, in the absence of Mersmab1, MERS-CoV pseudoviruses entered DPP4-expressing HEK293T cells efficiently, but the entry was blocked effectively by Mersmab1 (Fig. 3A). In control experiments, anti-SARS MAb did not mediate MERS-CoV pseudovirus entry into Fc receptor-expressing HEK293T cells or macrophages, nor did it block MERS-CoV pseudovirus entry into DPP4 receptor-expressing HEK293T cells (Fig. 3A). In another set of control experiments, we showed that neither the Fc nor the Fab portion of Mersmab1 could mediate MERS-CoV pseudovirus entry into Fc receptor-expressing HEK293T cells or macrophages (Fig. 3B),

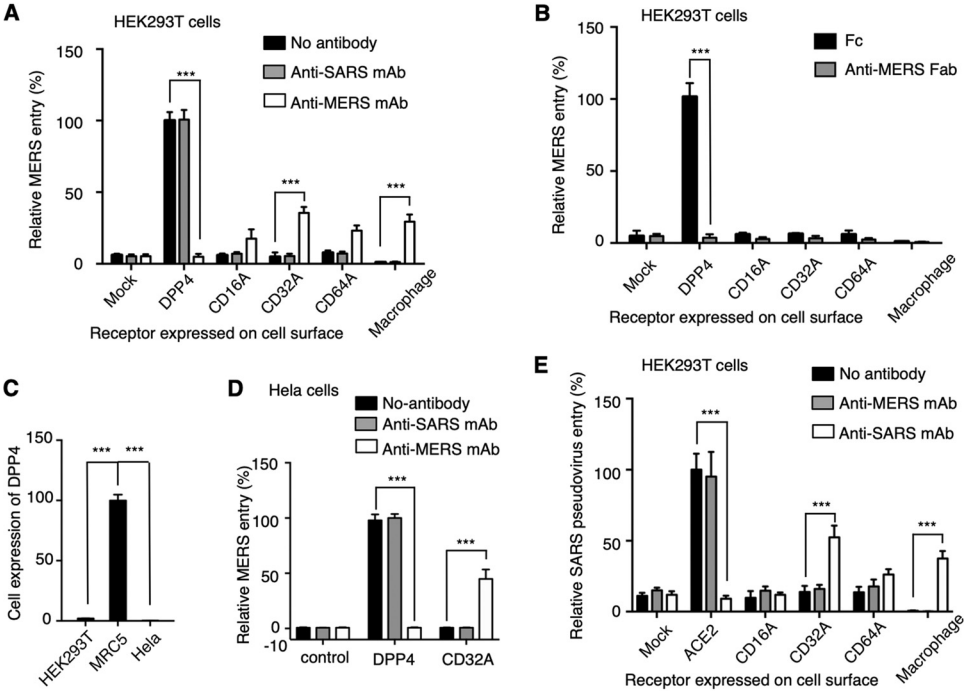

FIG 3 Antibody-dependent enhancement of coronavirus entry. (A) Antibody-mediated MERS-CoV pseudovirus entry into human cells. The human cells included HEK293T cells exogenously expressing DPP4, HEK293T cells exogenously expressing one of the Fc receptors (CD16A, CD32A, or CD64A), and macrophages (induced from THP-1 monocytes) endogenously expressing a mixture of Fc receptors. The antibody was Mersmab1. An anti-SARS MAb (i.e., 33G4) was used as a negative control. Efficiency of pseudovirus entry was characterized by luciferase activities accompanying entry. HEK293T cells not expressing any viral receptor or Fc receptor were used as a control. (B) Fc- or Fab-mediated MERS-CoV pseudovirus entry into human cells. The Fc or the Fab portion of Mersmab1 was used in MERS-CoV pseudovirus entry performed as for panel A. (C) Expression levels of DPP4 receptor in different cell lines. Total RNA was extracted from three different cell lines: HEK293T, MRC5, and HeLa. Then qRT-PCR was performed on the total RNAs from each cell line. The expression level of DPP4 in each cell line is defined as the ratio between the RNA of DPP4 and the RNA of glyceraldehyde-3-phosphate dehydrogenase (GAPDH). (D) Antibody-mediated MERS-CoV pseudovirus entry into HeLa cells that do not express DPP4 receptor. The experiments were performed in the same way as for panel A, except that HeLa cells replaced HEK293T cells. (E) Antibody-mediated SARS-CoV pseudovirus entry into human cells. DPP4 and Mersmab1 were replaced by ACE2 and 33G4, respectively. Mersmab1 was used as a negative control. All of the experiments were repeated at least three times, with similar results, and representative results are shown here. Error bars indicate SD ($n = 4$). Statistical analyses were performed as a one-tailed t test. ***, $P < 0.001$. RBD-specific MAbs mediate ADE of coronavirus entry while blocking viral-receptor-dependent coronavirus entry.

suggesting that both the Fc and Fab portions of anti-MERS MAb are required for antibody-mediated viral entry. The above-mentioned DPP4-expressing HEK293T cells were induced to exogenously express high levels of DPP4. To detect background expression levels of DPP4, we performed reverse transcription-quantitative PCR (qRT-PCR) on HEK293T cells. The result showed that HEK293T cells express very low levels of DPP4 (Fig. 3C). In comparison, MRC5 cells (human lung cells) express high levels of DPP4, whereas HeLa cells (human cervical cells) do not express DPP4 (Fig. 3C). Because of the comprehensive control experiments that we performed, the very low endogenous expression of DPP4 in HEK293T cells should not affect our conclusions. Nevertheless, we confirmed the above results using HeLa cells that do not express DPP4 (Fig. 3D). Overall, our results reveal that Mersmab1 mediates MERS-CoV entry into Fc receptor-expressing cells but blocks MERS-CoV entry into DPP4-expressing cells.

To expand the above-described observations to another coronavirus, we investigated ADE of SARS-CoV entry. We previously identified a SARS-CoV RBD-specific MAb, named 33G4, which binds to the ACE2-binding region of SARS-CoV RBD (49, 50); this MAb was examined for its potential capability to mediate ADE of SARS-CoV entry (Fig. 3E). The result showed that 33G4 mediated SARS-CoV pseudovirus entry into CD32A-expressing cells but blocked SARS-CoV pseudovirus entry into ACE2-expressing cells.

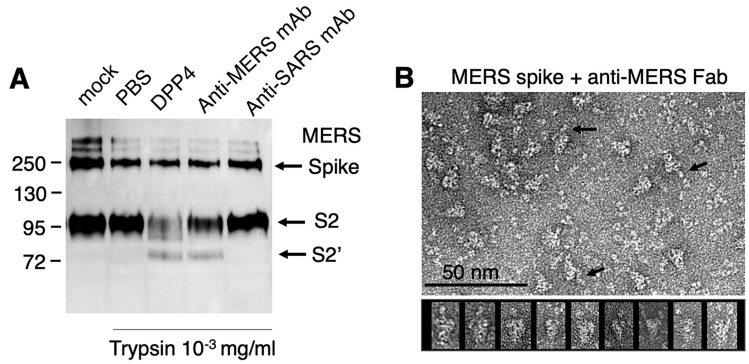

FIG 4 Antibody-induced conformational changes of coronavirus spike. (A) Purified MERS-CoV pseudoviruses were incubated with recombinant DPP4, MAb, or PBS and then treated with trypsin. Samples were subjected to Western blotting. MERS-CoV spike and its cleaved fragments (all of which contained a C-terminal C9 tag) were detected using an anti-C9 tag monoclonal antibody. Both DPP4 and Mersmab1 triggered conformational changes of MERS-CoV spike, allowing it to cleaved at the S2′ site by trypsin. (B) Negative-stain electron microscopic analysis of MERS-CoV S-e in complex with the Fab of Mersmab1. Both a field of particles and windows of individual particles are shown. Black arrows indicate S-e-bound Fabs. According to previous studies (18, 20, 21), the Fab-binding site on the trimeric S-e is accessible only when the RBD is in the standing-up position.

Therefore, both the MERS-CoV RBD-specific MAb and the SARS-CoV RBD-specific MAb can mediate the entry of the respective coronavirus into Fc receptor-expressing human cells while blocking the entry of the respective coronavirus into viral-receptor-expressing human cells. For the remainder of this study, we selected the MERS-CoV RBD-specific MAb Mersmab1 for in-depth analysis of ADE.

Molecular mechanism for antibody-dependent enhancement of coronavirus entry. To understand the molecular mechanism of ADE, we investigated whether Mersmab1 triggers any conformational change of MERS-CoV spike. It was shown previously that DPP4 binds to MERS-CoV spike and stabilizes the RBD in the standing-up position (Fig. 1A and B), resulting in a weakened spike structure and allowing the S2′ site to become exposed to proteases (51). We repeated this experiment: MERS-CoV pseudoviruses were incubated with DPP4 and then subjected to trypsin cleavage (Fig. 4A). The results showed that during the viral packaging process, virus surface-anchored MERS-CoV spike molecules were cleaved at the S1/S2 site by proprotein convertases; in the absence of DPP4, the spike molecules could not be cleaved further at the S2′ site by trypsin. These data suggest that only the S1/S2 site, and not the S2′ site, was accessible to proteases in the free form of the spike trimer. In the presence of DPP4, a significant amount of MERS-CoV spike molecules were cleaved at the S2′ site by trypsin, indicating that DPP4 binding triggered a conformational change of MERS-CoV spike to expose the S2′ site. Interestingly, we found that Mersmab1 binding also allowed MERS-CoV spike to be cleaved at the S2′ site by trypsin. As a negative control, the SARS-CoV RBD-specific MAb did not trigger MERS-CoV spike to be cleaved at the S2′ site by trypsin. Hence, like DPP4, Mersmab1 triggers a conformational change of MERS-CoV spike to expose the S2′ site for proteolysis.

We further analyzed the binding between Mersmab1 and MERS-CoV S-e using negative-stain electron microscopy (EM). We previously demonstrated through mutagenesis studies that Mersmab1 binds to the same receptor-binding region on MERS-CoV RBD as DPP4 does (Fig. 1C) (48). Because full-length Mersmab1 (which is a dimer) triggered aggregation of S-e (which is a trimer), we prepared the Fab part (which is a monomer) of Mersmab1, detected the binding between Fab and S-e (Fig. 2B), and used Fab in the negative-stain EM study. The results showed that Fab bound to the tip of the S-e trimer, where the RBD is located (Fig. 4B). Due to the limited resolution of negative-stain EM, we could not clearly see the conformation of the Fab-bound RBD. However, based on previous studies, the receptor-binding site on the RBD in the spike trimer is accessible only when the RBD is in the standing-up position (18, 20, 21). Hence,

the fact that the MAb binds to the receptor-binding region of the RBD in the spike trimer suggests that the RBD is in the standing-up state. Thus, the results from negative-stain EM and the proteolysis study are consistent with each other, supporting the idea that like DPP4, Mersmab1 stabilizes the RBD in the standing-up position and triggers a conformational change of the spike. Future study on the high-resolution cryo-EM structure of MERS-CoV S-e trimer complexed with Mersmab1 will be needed to provide detailed structural information for the Mersmab1-triggered conformational changes of MERS-CoV S-e.

To understand the pathways of Mersmab1-dependent MERS-CoV entry, we evaluated the potential impact of different proteases on MERS-CoV pseudovirus entry; these proteases are distributed along the viral entry pathway. First, proprotein convertase inhibitor (PPCi) was used for examining the role of proprotein convertases in the maturation of MERS-CoV spike and the impact of proprotein convertases on the ensuing Mersmab1-dependent viral entry (Fig. 5A). The results showed that when MERS-CoV pseudoviruses were produced from HEK293T cells in the presence of PPCi, the cleavage of MERS-CoV spike by proprotein convertases was significantly inhibited (Fig. 5B). In the absence of Mersmab1, MERS-CoV pseudoviruses packaged in the presence of PPCi entered DPP4-expressing human cells more efficiently than those packaged in the absence of PPCi (Fig. 5A). In the presence of Mersmab1, MERS-CoV pseudoviruses packaged in the presence of PPCi entered CD32A-expressing cells more efficiently than those packaged in the absence of PPCi (Fig. 5A). These data suggest that proprotein convertases play a role (albeit not as drastic as some other proteases; see below) in both DPP4-dependent and Mersmab1-dependent MERS-CoV entries. Second, cell surface protease TMPRSS2 (transmembrane serine protease 2) was introduced to human cells for evaluation of its role in Mersmab1-dependent viral entry (Fig. 5C). The results showed that in the absence of Mersmab1, TMPRSS2 enhanced MERS-CoV pseudovirus entry into DPP4-expressing cells, consistent with previous reports (36). In the presence of Mersmab1, TMPRSS2 also enhanced MERS-CoV pseudovirus entry into CD32A-expressing cells, suggesting that TMPRSS2 activates Mersmab1-dependent MERS-CoV entry. Third, lysosomal protease inhibitors were evaluated for the role of lysosomal proteases in Mersmab1-dependent viral entry (Fig. 5D). Two inhibitors were used, lysosomal acidification inhibitor Baf-A1 and cysteine protease inhibitor E64d. The results showed that lysosomal protease inhibitors blocked the DPP4-dependent viral entry pathway, consistent with previous reports (39). Lysosomal protease inhibitors also blocked the Mersmab1-dependent viral entry pathway, suggesting that lysosomal proteases play important roles in Mersmab1-dependent MERS-CoV entry. Taken together, the DPP4-dependent and Mersmab1-dependent MERS-CoV entries can both be activated by proprotein convertases, cell surface proteases, and lysosomal proteases; hence, the same pathways are shared by DPP4-dependent and Mersmab1-dependent MERS-CoV entries.

Antibody dosages for antibody-dependent enhancement of coronavirus entry. To determine the range of Mersmab1 dosages in ADE, MERS-CoV pseudovirus entry was performed in the presence of different concentrations of Mersmab1. Three types of human HEK293T cells were used: HEK293T cells exogenously expressing DPP4 only, CD32A only, or both DPP4 and CD32A. Accordingly, three different sets of results were obtained. First, as the amount of Mersmab1 increased, viral entry into DPP4-expressing HEK293T cells continuously dropped (Fig. 6A). This result reveals that Mersmab1 blocks the DPP4-dependent viral entry pathway by outcompeting DPP4 for binding to MERS-CoV spike. Second, as the amount of Mersmab1 increased, viral entry into CD32A-expressing HEK293T cells first increased and then decreased (Fig. 6A). The turning point was about 100 ng/ml of Mersmab1. A likely explanation for this result is as follows: at low concentrations, more MAb molecules enhance the indirect interactions between MERS-CoV spike and the Fc receptor; at high concentrations, MAb molecules saturate the cell surface Fc receptor molecules and then further bind to MERS-CoV spike and block the indirect interactions between MERS-CoV spike and the Fc receptor. Third, as the amount of Mersmab1 increased, viral entry into cells expressing both DPP4 and

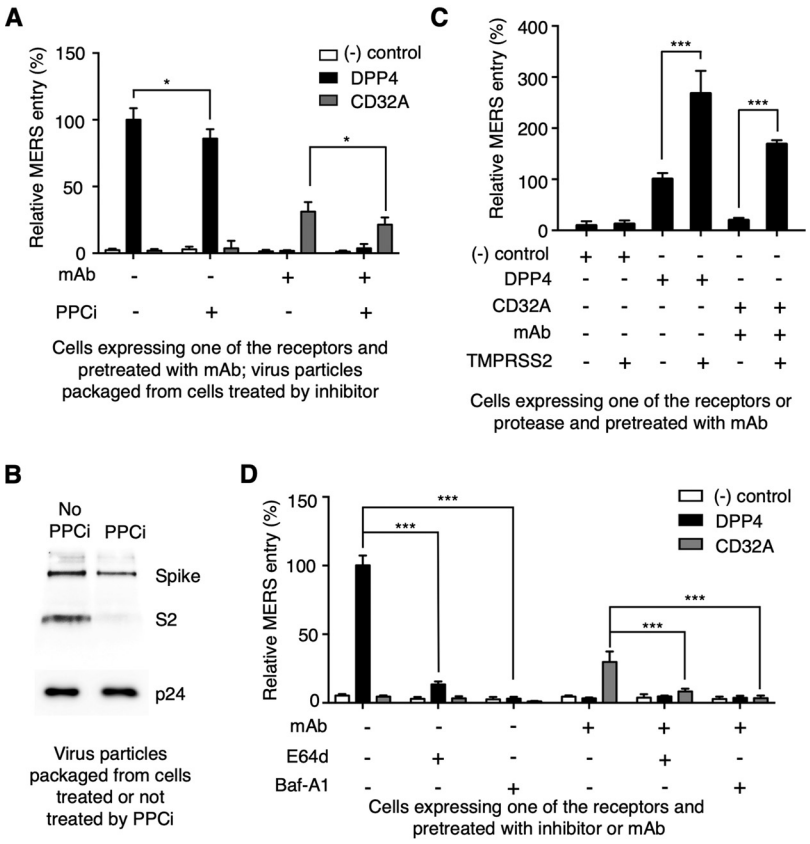

FIG 5 Pathways for antibody-dependent enhancement of coronavirus entry. (A) Impact of proprotein convertases on ADE of MERS-CoV entry. During packaging of MERS-CoV pseudoviruses, HEK293T cells were treated with proprotein convertase inhibitor (PPCi). The MERS-CoV pseudoviruses packaged in the presence of PPCi were then subjected to MERS-CoV pseudovirus entry into HEK293T cells expressing either DPP4 receptor or CD32A receptor. (B) Western blot of MERS-CoV pseudoviruses packaged in the presence or absence of PPCi. MERS-CoV spike protein was detected using anti-C9 antibody targeting its C-terminal C9 tag. As an internal control, another viral protein, p24, was detected using an anti-p24 antibody. (C) Impact of cell surface proteases on ADE of MERS-CoV entry. HEK293T cells exogenously expressing TMPRSS2 (which is a common cell surface protease) were subjected to MERS-CoV pseudovirus entry. TMPRSS2 enhanced both the DPP4-dependent and antibody-dependent entry pathways. (D) Impact of lysosomal proteases on ADE of MERS-CoV entry. HEK293T cells exogenously expressing DPP4 or CD32A were pretreated with one of the lysosomal protease inhibitors E64d and Baf-A1 and then subjected to MERS-CoV pseudovirus entry. Lysosomal protease inhibitors blocked both the DPP4-dependent and antibody-dependent entry pathways. HEK293T cells not expressing DPP4 or CD32A were used as a negative control. All of the experiments were repeated at least three times, with similar results, and representative results are shown. Error bars indicate SD ($n = 4$). Statistical analyses were performed as a one-tailed t test. ***, $P < 0.001$; *, $P < 0.05$. Antibody-dependent and DPP4-dependent viral entries share the same pathways.

CD32A first dropped, then increased, and finally dropped again (Fig. 6B). This result is the cumulative effect of the previous two results. It reveals that when both DPP4 and CD32A are present on host cell surface, Mersmab1 inhibits viral entry (by blocking the DPP4-dependent entry pathway) at low concentrations, promotes viral entry (by enhancing the CD32A-dependent entry pathway) at intermediate concentrations, and inhibits viral entry (by blocking both the DPP4- and CD32A-dependent entry pathways) at high concentrations. We further confirmed the above-described results using MRC5 cells, which are human lung cells endogenously expressing DPP4 (Fig. 6C and D). Therefore, ADE of MERS-CoV entry depends on the range of Mersmab1 dosages as well as expressions of the viral and Fc receptors on cell surfaces.

DISCUSSION

ADE of viral entry has been observed and studied extensively in flaviviruses, particularly dengue virus (3–6). It has also been observed in HIV and Ebola viruses

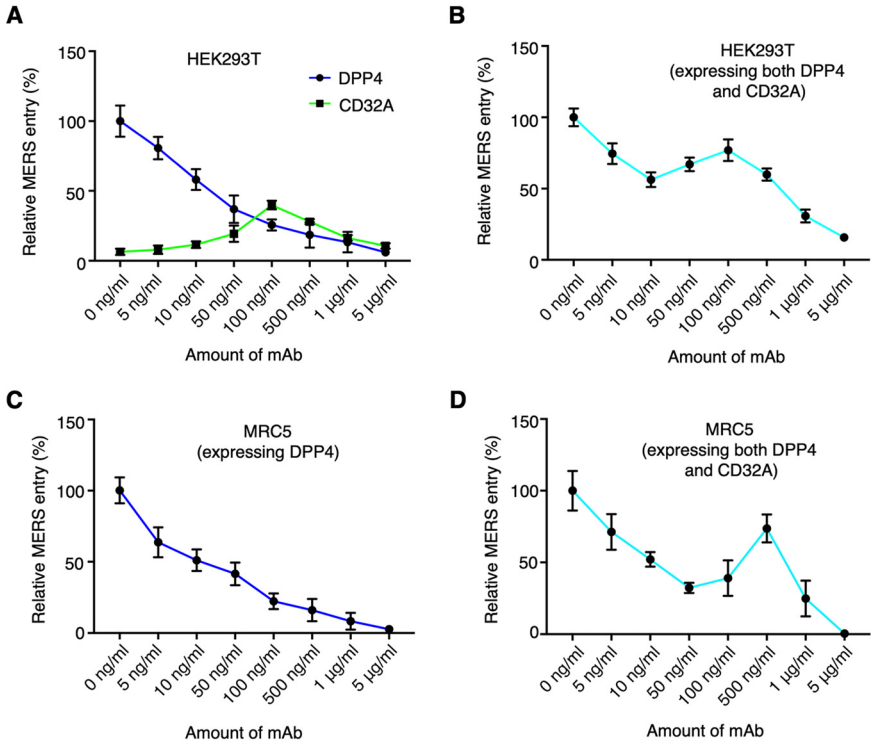

FIG 6 Antibody dosages for antibody-dependent enhancement of coronavirus entry. (A) Impact of antibody dosages on MERS-CoV pseudovirus entry into HEK293T cells exogenously expressing either DPP4 or CD32A. MAb blocks the DPP4-dependent entry pathway; it enhances the antibody-dependent entry pathway at lower concentrations and blocks it at higher concentrations. (B) Impact of antibody dosages on MERS-CoV pseudovirus entry into HEK293T cells exogenously expressing both DPP4 and CD32A. In the presence of both DPP4 and CD32A, MAb blocks viral entry at low concentrations, enhances viral entry at intermediate concentrations, and blocks viral entry at high concentrations. (C) Same experiment as in panel A, except that MRC5 cells replaced HEK293T cells. Here MRC5 cells express DPP4 receptor endogenously. (D) Same experiment as in panel B, except that MRC5 cells replaced HEK293T cells. Here MRC5 cells endogenously express DPP4 and exogenously express CD32A. Please refer to the text for more detailed explanations. All of the experiments were repeated at least three times, with similar results, and representative results are shown. Error bars indicate SD ($n = 4$).

(7–10). For these viruses, it has been proposed that primary viral infections of hosts led to production of antibodies that are subneutralizing or nonneutralizing for secondary viral infections; these antibodies cannot completely neutralize secondary viral infections but instead guide virus particles to enter Fc receptor-expressing cells. ADE can lead to worsened symptoms in secondary viral infections, causing major concerns for epidemiology. ADE is also a major concern for vaccine design and antibody-based drug therapy, since antibodies generated or used in these procedures may lead to ADE. ADE has been observed in coronaviruses for decades, but the molecular mechanisms are unknown. Recent advances in understanding of the receptor recognition and cell entry mechanisms of coronaviruses have allowed us to use coronaviruses as a model system for studying ADE.

In this study, we first demonstrated that a MERS-CoV RBD-specific neutralizing MAb binds to the RBD region of MERS-CoV spike and further showed that the MAb mediates MERS-CoV pseudovirus entry into Fc receptor-expressing human cells. Moreover, a SARS-CoV RBD-specific neutralizing MAb mediates ADE of SARS-CoV pseudovirus entry. These results demonstrated that ADE of coronaviruses is mediated by neutralizing MAbs that target the RBD of coronavirus spikes. In addition, the same coronavirus strains that led to the production of fully neutralizing MAbs can be mediated to go through ADE by these neutralizing MAbs. Our results differ from previously observed ADE of flaviviruses in which primary infections and secondary infections are caused by two different viral strains and in which ADE-mediating MAbs are only subneutralizing

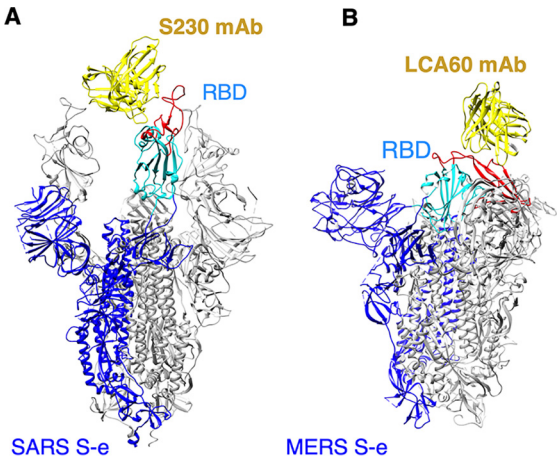

FIG 7 Two previously published structures of coronavirus spike proteins complexed with antibody. (A) SARS-CoV S-e complexed with S230 MAb (PDB code 6NB7). The antibody binds to the side of the RBD, away from the viral-receptor-binding site, stabilizes the RBD in the lying-down state, and hence does not trigger conformational changes of SARS-CoV S-e. (B) MERS-CoV S-e complexed with LCA60 MAb (PDB code 6NB4). The antibody binds to the viral-receptor-binding site in the RBD, stabilizes the RBD in the standing-up state, and hence triggers conformational changes of MERS-CoV S-e.

or nonneutralizing for secondary viral infections (3–6). Therefore, our study expands the concept of ADE of viral entry.

We then examined the molecular mechanism for ADE of coronavirus entry. We showed that the MAb binds to the tip of MERS-CoV spike trimer, where the RBD is located. MAb binding likely stabilizes the RBD in the standing-up position, triggers a conformational change of MERS-CoV spike, and exposes the previously inaccessible S2′ site to proteases. During the preparation of the manuscript, a newly published study demonstrated that a SARS-CoV RBD-specific MAb (named S230) bound to the ACE2-binding region in SARS-CoV RBD, stabilized the RBD in the standing-up position, and triggered conformational changes of SARS-CoV spike (Fig. 7A) (52). In contrast, a MERS-CoV RBD-specific MAb (named LCA60) bound to the side of MERS-CoV RBD, away from the DPP4-binding region, stabilized the RBD in the lying-down position, and did not trigger conformational changes of MERS-CoV spike (Fig. 7B). These published results are consistent with our results regarding Mersmab1-triggered conformational changes of MERS-CoV spike, together suggesting that in order to trigger conformational changes of coronavirus spikes, MAbs need to bind to the receptor-binding region in their RBD and stabilize the RBD in the standing-up position. Moreover, our study revealed that ADE of MERS-CoV entry follows the same entry pathways as DPP4-dependent MERS-CoV entry. Specifically, proprotein convertases partially activate MERS-CoV spike. If cell surface proteases are present, MERS-CoV spike can be further activated and fuse membranes on the cell surface; otherwise, MERS-CoV enters endosomes and lysosomes, where lysosomal proteases activate MERS-CoV spike for membrane fusion. Taken together, our results show that RBD-specific neutralizing MAbs bind to the same region on coronavirus spikes as viral receptors do, trigger conformational changes of the spikes as viral receptors do, and mediate ADE through the same pathways as viral-receptor-dependent viral entry. In other words, RBD-specific neutralizing MAbs mediate ADE of coronavirus entry by functionally mimicking viral receptors.

Finally, we analyzed ADE of coronavirus entry at different antibody dosages. MERS-CoV entry into cells expressing both viral and Fc receptors demonstrates complex MAb-dosage-dependent patterns. As the concentration of MAb increases, (i) viral entry into DPP4-expressing cells is inhibited more efficiently because MAb binds to the spike and blocks the DPP4-dependent entry pathway, (ii) viral entry into Fc receptor-expressing cells is first enhanced and then inhibited because MAb binds to the Fc receptor to enhance the ADE pathway until the Fc receptor molecules are saturated, and (iii) viral entry into cells

expressing both DPP4 and Fc receptor is first inhibited, then enhanced, and finally inhibited again because of the cumulative effects of the previous two patterns. In other words, for viral entry into cells expressing both DPP4 and Fc receptor, there exists a balance between the DPP4-dependent and antibody-dependent entry pathways that can be shifted and determined by MAb dosages. Importantly, ADE occurs only at intermediate MAb dosages. Our study explains an earlier observation that ADE of dengue viruses occurs only at certain concentrations of MAb (5). While many human tissues express either DPP4 or Fc receptor, a few of them, most notably placenta, express both of them (53, 54). For other viruses that use viral receptors different from DPP4, there may also be human tissues where the viral receptor and Fc receptor are both expressed. The expression levels of these two receptors in specific tissue cells likely are determinants of MAb dosages at which ADE would occur in these tissues. Other determinants of ADE-enabling MAb dosages may include the binding affinities of the MAb for the viral and Fc receptors. Overall, our study suggests that ADE of viruses depends on antibody dosages, tissue-specific expressions of viral and Fc receptors, and some intrinsic features of the antibody.

Our findings not only reveal a novel molecular mechanism for ADE of coronaviruses but also provide general guidelines on viral vaccine design and antibody-based antiviral drug therapy. As we have shown here, RBD-specific neutralizing MAbs may mediate ADE of viruses by mimicking the functions of viral receptors. Neutralizing MAbs targeting other parts of viral spikes would be less likely to mediate ADE if they do not trigger the conformational changes of the spikes. Hence, to reduce the likelihood of ADE, spike-based subunit vaccines lacking the RBD can be designed to prevent viral infections. Based on the same principle, neutralizing MAbs targeting other parts of the spike can be selected to treat viral infections. Moreover, as already discussed, our study stresses on the importance of choosing antibody dosages that do not cause ADE and points out that different tissue cells should be closely monitored for potential ADE at certain antibody dosages.

The *in vitro* systems used in this study provide a model framework for ADE. Future research using *in vivo* systems is needed to further confirm these results. Our previous study showed that a humanized version of Mersmab1 efficiently protected human DPP4-transgenic mice from live MERS-CoV challenges (48, 55), suggesting that given the antibody dosages used in this previous study as well as the binding affinity of the MAb for human DPP4, the receptor-dependent pathway of MERS-CoV entry dominated over ADE *in vivo*. Thus, future *in vivo* studies may need to screen for a wide range of antibody dosages and also for a variety of tissues with different ratios of DPP4 and Fc receptor expressions. Although ADE has not been observed for MERS-CoV *in vivo*, our study suggests that ADE occurs under some specific conditions *in vivo*, depending on the antibody dosages, binding affinity of the MAb for DPP4, and tissue expressions of DPP4 and Fc receptor. Moreover, the mechanism that we have identified for ADE of MERS-CoV *in vitro* may account for the ADE observed *in vivo* for other coronaviruses, such as SARS-CoV and feline coronavirus (42–47). Overall, our study reveals complex roles of antibodies in viral entry and can guide future vaccine design and antibody-based drug therapy.

MATERIALS AND METHODS

Cell lines and plasmids. HEK293T cells and HEK293F cells (human embryonic kidney cells), HeLa cells (human cervical cells), and MRC5 cells (human lung cells) were obtained from the American Type Culture Collection (ATCC). HEK293-gamma chain cells (human embryonic kidney cells) were constructed previously (56). These cells were cultured in Dulbecco's modified Eagle medium (DMEM) supplemented with 10% fetal bovine serum (FBS), 2 mM L-glutamine, 100 U/ml of penicillin, and 100 μg/ml of streptomycin. THP-1 cells (human macrophages) were obtained from the ATCC and were cultured in RPMI culture medium (Invitrogen) containing 10% heat-inactivated FBS and supplemented with 10 mM HEPES, 1 mM pyruvate, 2.5 g/liter of D-glucose, 50 pM β-mercaptoethanol, and 100 μg/ml of streptomycin.

For induction of macrophages, human monocytic THP-1 cells were treated with 150 nM phorbol 12-myristate 13-acetate for 24 h, followed by 24 h of incubation in RPMI medium (57) before experiments.

The full-length genes of MERS-CoV spike (GenBank accession number AFS88936.1), SARS-CoV spike (GenBank accession number AFR58742), human DPP4 (GenBank accession number NM_001935.4), and human ACE2 (GenBank accession number NM_001371415.1) were synthesized (GenScript Biotech). Three

Fc receptor genes, human CD16A (GenBank accession number NM_000569.7), human CD32A (GenBank accession number NM_001136219.3), and human CD64A (GenBank accession number NM_000566.3), were cloned previously (58, 59). For protein expressions on cell surfaces or pseudovirus surfaces, the above-named genes were subcloned into the pcDNA3.1(+) vector (Life Technologies) with a C-terminal C9 tag.

Protein purification and antibody preparation. For ELISA and negative-stain electron microscopic study, recombinant MERS-CoV spike ectodomain (S-e) was prepared. The MERS-CoV S-e (residues 1 to 1294) was subcloned into pCMV vector; it contained a C-terminal GCN4 trimerization tag and a His_6 tag. To stabilize S-e in the prefusion conformation, we followed the procedure from a previous study by introducing mutations to the S1/S2 protease cleavage site (RSVR748-751ASVA) and the S2 region (V1060P and L1061P) (21). MERS-CoV S-e was expressed in HEK293F cells using a FreeStyle 293 mammalian cell expression system (Life Technologies). Briefly, HEK293F cells were transfected with the plasmid encoding MERS-CoV S-e and cultured for 3 days. The protein was harvested from the cell culture medium, purified sequentially on a nickel-nitrilotriacetic aid (Ni-NTA) column and Superdex200 gel filtration column (GE Healthcare), and stored in a buffer containing 20 mM Tris (pH 7.2) and 200 mM NaCl. The ectodomain of human DPP4 was expressed and purified as previously described (39). Briefly, DPP4 ectodomain (residues 39 to 766) containing an N-terminal human CD5 signal peptide and a C-terminal His_6 tag was expressed in insect cells using the Bac-to-Bac expression system (Life Technologies), secreted to cell culture medium, and purified in the same way as MERS-CoV S-e.

Both the MERS-CoV RBD-specific MAb (i.e., Mersmab1) and SARS-CoV RBD-specific MAb (i.e., 33G4) were purified as previously described (48, 49). Briefly, hybridoma cells expressing the MAb were injected into the abdomens of mice. After 7 to 10 days, the mouse ascites containing the MAb were collected. The MAb was then purified using a protein A column (GE Healthcare). Fab of Mersmab1 antibody was prepared using immobilized papain beads (Thermo Fisher Scientific) according to the manufacturer's manual. Briefly, Mersmab1 antibody was incubated with immobilized papain beads in digestion buffer (20 mM sodium phosphate, 10 mM EDTA, 20 mM L-cysteine HCl [pH 7.0]) in a shaking water bath at 37°C overnight. After digestion, the reaction was stopped with 10 mM Tris HCl (pH 7.5), and the supernatant was collected through centrifugation at 12,000 × *g* for 15 min. Fab was then separated from undigested IgG and Fc using a protein A column (GE HealthCare).

ELISA. The binding affinity between MAb and MERS-CoV S-e or RBD was measured using ELISA as previously described (60). Briefly, ELISA plates were precoated with MAb (350 nM) at 37°C for 1 h. After blocking with 1% bovine serum albumin (BSA) at 37°C for 1 h, MERS-CoV S-e or RBD (300 nM or gradient concentrations as specified in Fig. 2) was added to the plates and incubated with MAb at 37°C for 1 h. After washes with phosphate-buffered saline (PBS), the plates were incubated with anti-His_6 antibody (Santa Cruz) at 37°C for 1 h. Then the plates were washed with PBS and incubated with horseradish peroxidase (HRP)-conjugated goat anti-mouse IgG antibody (1:5,000) at 37°C for 1 h. After more washes with PBS, the enzymatic reaction was carried out using ELISA substrate (Life Technologies) and stopped with 1 M H_2SO_4. Absorbance at 450 nm (A_{450}) was measured using a Tecan Infinite M1000 PRO microplate reader (Tecan Group Ltd.). Five replicates were done for each sample. PBS was used as a negative control.

Flow cytometry cell-binding assay. Flow cytometry was performed as previously described (22). Briefly, HEK293T cells exogenously expressing DPP4 or one of the Fc receptors were incubated with MERS-CoV S-e (40 μg/ml) and MAb (50 μg/ml) (both of which contained a C-terminal His_6 tag) at room temperature for 30 min, followed by incubation with fluorescein phycoerythrin (PE)-labeled anti-His_6 probe antibody for another 30 min. The cells then were analyzed using fluorescence-activated cell sorting (FACS).

Pseudovirus entry assay. The coronavirus spike-mediated pseudovirus entry assay was carried out as previously described (61, 62). Briefly, for pseudovirus packaging, HEK293T cells were cotransfected with a plasmid carrying an Env-defective, luciferase-expressing HIV type 1 genome (pNL4–3.luc.R-E-) and a plasmid encoding MERS-CoV or SARS-CoV spike. Pseudoviruses were harvested and purified using a sucrose gradient ultracentrifugation at 40,000 × *g* 72 h after transfection and then used to enter the target cells. To detect pseudovirus entry, pseudoviruses and cells were incubated for 5 h at 37°C, and then medium was changed and cells were incubated for an additional 60 h. Cells were then washed with PBS and lysed. Aliquots of cell lysates were transferred to Optiplate-96 (PerkinElmer), followed by addition of luciferase substrate. Relative light unites (RLUs) were measured using an EnSpire plate reader (PerkinElmer). All the measurements were carried out in four replicates. To inhibit proprotein convertases during packaging of MERS-CoV pseudoviruses, 50 nM proprotein convertase inhibitor (PPCi) Dec-RVKR-CMK (Enzo Life Sciences) was added to the cell culture medium 5 h posttransfection, before the packaged pseudoviruses were purified as described above. Inhibition of pseudovirus entry using various protease inhibitors was carried out as described previously (63). Briefly, cells were pretreated with 50 nM proprotein convertase inhibitor Dec-RVKR-CMK (Enzo Life Sciences), 100 nM camostat mesylate (Sigma-Aldrich), 100 nM bafilomycin A1 (Baf-A1) (Sigma-Aldrich), and 50 nM E64d (Sigma-Aldrich) at 37°C for 1 h or 500 ng/ml antibody for 5 min. The above-described cells were then used for pseudovirus entry assay.

Isolation and quantification of cell surface receptor proteins. To examine the expression levels of receptor proteins in cell membranes, the cells expressing the receptor were harvested and all membrane-associated proteins were extracted using a membrane protein extraction kit (Thermo Fisher Scientific). Briefly, cells were centrifuged at 300 × *g* for 5 min and washed with cell wash solution twice. The cell pellets were resuspended in 0.75 ml of permeabilization buffer and incubated at 4°C for 10 min. The supernatant containing cytosolic proteins was removed after centrifugation at 16,000 × *g* for 15 min. The pellets containing membrane-associated proteins were resuspended in 0.5 ml of solubilization buffer and incubated at 4°C for 30 min. After centrifugation at 16,000 × *g* for 15 min, the membrane-associated

proteins from the supernatant were transferred to a new tube. The expression level of membrane-associated C9-tagged receptor proteins among all membrane-associated proteins was then measured using Western blot analysis and further used for normalizing the results from flow cytometry cell-binding assays and pseudovirus entry assays.

Extraction of total RNA and qRT-PCR. Total RNAs of cells were extracted using TRIzol reagent according to the manufacturer's manual. Briefly, TRIzol was added to the cell lysate, and then chloroform and phenol-chloroform were added to precipitate RNA. The RNA pellets were washed using ethanol, solubilized in diethyl pyrocarbonate (DEPC)-treated water, and then reverse transcribed using murine leukemia virus (MLV) reverse transcriptase (Promega) and oligo(dT) primers (Promega). Quantitative PCR on DPP4 RNA was performed using DPP4-specific primers and a SYBR qPCR kit (Bio-Rad) in a CFX qPCR instrument (Bio-Rad). Glyceraldehyde-3-phosphate dehydrogenase (GAPDH) RNA was used as a control. The primers are as follows: for DPP4, forward, 5′-AGTGGCGTGTTCAAGTGTGG-3′, and reverse, 5′-CAAG GTTGTCTTCTGGAGTTGG-3′; for GAPDH, forward, 5′-GGAAGGTGAAGGTCGGAGTCAACGG-3′, and reverse, 5′-CTCGCTCCTGGAAGATGGTGATGGG-3′.

Proteolysis assay. Purified MERS-CoV pseudoviruses were incubated with 67 μg/ml of recombinant DPP4, 67 μg/ml of MAb, or PBS at 37°C for 30 min and then treated with 10^{-3} mg/ml of tosylsulfonyl phenylalanyl chloromethyl ketone (TPCK)-treated trypsin on ice for 20 min. Samples were subjected to Western blotting. MERS-CoV spike and its cleaved fragments (which contained a C-terminal C9 tag) were detected using an anti-C9 tag monoclonal antibody (Santa Cruz Biotechnology).

Negative-stain electron microscopy. Samples were diluted to a final concentration of 0.02 mg/ml in PBS and loaded onto glow-discharged 400-mesh carbon grids (Electron Microscopy Sciences). The grids were stained with 0.75% uranyl formate. All micrographs were acquired using a Tecnai G2 Spirit BioTWIN at 120 keV (FEI Company) and an Eagle 4-megapixel charge-coupled-device (CCD) camera at 6,000 × nominal magnification at the University of Minnesota.

ACKNOWLEDGMENTS

We thank Matthew Aliota for comments.

This work was supported by NIH grants R01AI089728 (to F.L), R01AI110700 (to F.L.), and R01AI139092 (to L.D. and F.L.).

REFERENCES

1. Tirado SM, Yoon KJ. 2003. Antibody-dependent enhancement of virus infection and disease. Viral Immunol 16:69–86. https://doi.org/10.1089/088282403763635465.
2. Takada A, Kawaoka Y. 2003. Antibody-dependent enhancement of viral infection: molecular mechanisms and in vivo implications. Rev Med Virol 13:387–398. https://doi.org/10.1002/rmv.405.
3. Guzman MG, Alvarez M, Rodriguez-Roche R, Bernardo L, Montes T, Vazquez S, Morier L, Alvarez A, Gould EA, Kouri G, Halstead SB. 2007. Neutralizing antibodies after infection with dengue 1 virus. Emerg Infect Dis 13:282–286. https://doi.org/10.3201/eid1302.060539.
4. Dejnirattisai W, Jumnainsong A, Onsirisakul N, Fitton P, Vasanawathana S, Limpitikul W, Puttikhunt C, Edwards C, Duangchinda T, Supasa S, Chawansuntati K, Malasit P, Mongkolsapaya J, Screaton G. 2010. Cross-reacting antibodies enhance dengue virus infection in humans. Science 328:745–748. https://doi.org/10.1126/science.1185181.
5. Katzelnick LC, Gresh L, Halloran ME, Mercado JC, Kuan G, Gordon A, Balmaseda A, Harris E. 2017. Antibody-dependent enhancement of severe dengue disease in humans. Science 358:929–932. https://doi.org/10.1126/science.aan6836.
6. Whitehead SS, Blaney JE, Durbin AP, Murphy BR. 2007. Prospects for a dengue virus vaccine. Nat Rev Microbiol 5:518–528. https://doi.org/10.1038/nrmicro1690.
7. Willey S, Aasa-Chapman MMI, O'Farrell S, Pellegrino P, Williams I, Weiss RA, Neil SJD. 2011. Extensive complement-dependent enhancement of HIV-1 by autologous non-neutralising antibodies at early stages of infection. Retrovirology 8:16. https://doi.org/10.1186/1742-4690-8-16.
8. Beck Z, Prohaszka Z, Fust G. 2008. Traitors of the immune system-enhancing antibodies in HIV infection: their possible implication in HIV vaccine development. Vaccine 26:3078–3085. https://doi.org/10.1016/j.vaccine.2007.12.028.
9. Takada A, Watanabe S, Okazaki K, Kida H, Kawaoka Y. 2001. Infectivity-enhancing antibodies to Ebola virus glycoprotein. J Virol 75:2324–2330. https://doi.org/10.1128/JVI.75.5.2324-2330.2001.
10. Takada A, Feldmann H, Ksiazek TG, Kawaoka Y. 2003. Antibody-dependent enhancement of Ebola virus infection. J Virol 77:7539–7544. https://doi.org/10.1128/jvi.77.13.7539-7544.2003.
11. Perlman S, Netland J. 2009. Coronaviruses post-SARS: update on replication and pathogenesis. Nat Rev Microbiol 7:439–450. https://doi.org/10.1038/nrmicro2147.
12. Enjuanes L, Almazan F, Sola I, Zuniga S. 2006. Biochemical aspects of coronavirus replication and virus-host interaction. Annu Rev Microbiol 60:211–230. https://doi.org/10.1146/annurev.micro.60.080805.142157.
13. Zaki AM, van Boheemen S, Bestebroer TM, Osterhaus A, Fouchier R. 2012. Isolation of a novel coronavirus from a man with pneumonia in Saudi Arabia. N Engl J Med 367:1814–1820. https://doi.org/10.1056/NEJMoa1211721.
14. Ksiazek TG, Erdman D, Goldsmith CS, Zaki SR, Peret T, Emery S, Tong SX, Urbani C, Comer JA, Lim W, Rollin PE, Dowell SF, Ling AE, Humphrey CD, Shieh WJ, Guarner J, Paddock CD, Rota P, Fields B, DeRisi J, Yang JY, Cox N, Hughes JM, LeDuc JW, Bellini WJ, Anderson LJ. 2003. A novel coronavirus associated with severe acute respiratory syndrome. N Engl J Med 348:1953–1966. https://doi.org/10.1056/NEJMoa030781.
15. Peiris JSM, Lai ST, Poon LLM, Guan Y, Yam LYC, Lim W, Nicholls J, Yee WKS, Yan WW, Cheung MT, Cheng VCC, Chan KH, Tsang DNC, Yung RWH, Ng TK, Yuen KY. 2003. Coronavirus as a possible cause of severe acute respiratory syndrome. Lancet 361:1319–1325. https://doi.org/10.1016/S0140-6736(03)13077-2.
16. de Groot RJ, Baker SC, Baric RS, Brown CS, Drosten C, Enjuanes L, Fouchier RA, Galiano M, Gorbalenya AE, Memish ZA, Perlman S, Poon LL, Snijder EJ, Stephens GM, Woo PC, Zaki AM, Zambon M, Ziebuhr J. 2013. Middle East respiratory syndrome coronavirus (MERS-CoV): announcement of the Coronavirus Study Group. J Virol 87:7790–7792. https://doi.org/10.1128/JVI.01244-13.
17. Li F. 2016. Structure, function, and evolution of coronavirus spike proteins. Annu Rev Virol 3:237–261. https://doi.org/10.1146/annurev-virology-110615-042301.
18. Yuan Y, Cao D, Zhang Y, Ma J, Qi J, Wang Q, Lu G, Wu Y, Yan J, Shi Y, Zhang X, Gao GF. 2017. Cryo-EM structures of MERS-CoV and SARS-CoV spike glycoproteins reveal the dynamic receptor binding domains. Nat Commun 8:15092. https://doi.org/10.1038/ncomms15092.
19. Shang J, Zheng Y, Yang Y, Liu C, Geng Q, Luo C, Zhang W, Li F. 2018. Cryo-EM structure of infectious bronchitis coronavirus spike protein reveals structural and functional evolution of coronavirus spike proteins. PLoS Pathog 14:e1007009. https://doi.org/10.1371/journal.ppat.1007009.
20. Song W, Gui M, Wang X, Xiang Y. 2018. Cryo-EM structure of the SARS

coronavirus spike glycoprotein in complex with its host cell receptor ACE2. PLoS Pathog 14:e1007236. https://doi.org/10.1371/journal.ppat.1007236.
21. Pallesen J, Wang N, Corbett KS, Wrapp D, Kirchdoerfer RN, Turner HL, Cottrell CA, Becker MM, Wang L, Shi W, Kong WP, Andres EL, Kettenbach AN, Denison MR, Chappell JD, Graham BS, Ward AB, McLellan JS. 2017. Immunogenicity and structures of a rationally designed prefusion MERS-CoV spike antigen. Proc Natl Acad Sci U S A 114:E7348–E7357. https://doi.org/10.1073/pnas.1707304114.
22. Shang J, Zheng Y, Yang Y, Liu C, Geng Q, Tai W, Du L, Zhou Y, Zhang W, Li F. 2018. Cryo-electron microscopy structure of porcine deltacoronavirus spike protein in the prefusion state. J Virol 92:e01556-17. https://doi.org/10.1128/JVI.01556-17.
23. Walls AC, Tortorici MA, Bosch BJ, Frenz B, Rottier PJ, DiMaio F, Rey FA, Veesler D. 2016. Cryo-electron microscopy structure of a coronavirus spike glycoprotein trimer. Nature 531:114–117. https://doi.org/10.1038/nature16988.
24. Walls AC, Tortorici MA, Frenz B, Snijder J, Li W, Rey FA, DiMaio F, Bosch BJ, Veesler D. 2016. Glycan shield and epitope masking of a coronavirus spike protein observed by cryo-electron microscopy. Nat Struct Mol Biol 23:899–905. https://doi.org/10.1038/nsmb.3293.
25. Kirchdoerfer RN, Cottrell CA, Wang N, Pallesen J, Yassine HM, Turner HL, Corbett KS, Graham BS, McLellan JS, Ward AB. 2016. Pre-fusion structure of a human coronavirus spike protein. Nature 531:118–121. https://doi.org/10.1038/nature17200.
26. Li F. 2015. Receptor recognition mechanisms of coronaviruses: a decade of structural studies. J Virol 89:1954–1964. https://doi.org/10.1128/JVI.02615-14.
27. Li WH, Moore MJ, Vasilieva N, Sui JH, Wong SK, Berne MA, Somasundaran M, Sullivan JL, Luzuriaga K, Greenough TC, Choe H, Farzan M. 2003. Angiotensin-converting enzyme 2 is a functional receptor for the SARS coronavirus. Nature 426:450–454. https://doi.org/10.1038/nature02145.
28. Raj VS, Mou HH, Smits SL, Dekkers DHW, Muller MA, Dijkman R, Muth D, Demmers JAA, Zaki A, Fouchier RAM, Thiel V, Drosten C, Rottier PJM, Osterhaus A, Bosch BJ, Haagmans BL. 2013. Dipeptidyl peptidase 4 is a functional receptor for the emerging human coronavirus-EMC. Nature 495:251–254. https://doi.org/10.1038/nature12005.
29. Li F, Li WH, Farzan M, Harrison SC. 2005. Structure of SARS coronavirus spike receptor-binding domain complexed with receptor. Science 309:1864–1868. https://doi.org/10.1126/science.1116480.
30. Lu G, Hu Y, Wang Q, Qi J, Gao F, Li Y, Zhang Y, Zhang W, Yuan Y, Bao J, Zhang B, Shi Y, Yan J, Gao GF. 2013. Molecular basis of binding between novel human coronavirus MERS-CoV and its receptor CD26. Nature 500:227–231. https://doi.org/10.1038/nature12328.
31. Belouzard S, Millet JK, Licitra BN, Whittaker GR. 2012. Mechanisms of coronavirus cell entry mediated by the viral spike protein. Viruses 4:1011–1033. https://doi.org/10.3390/v4061011.
32. Heald-Sargent T, Gallagher T. 2012. Ready, set, fuse! The coronavirus spike protein and acquisition of fusion competence. Viruses 4:557–580. https://doi.org/10.3390/v4040557.
33. Bertram S, Glowacka I, Muller MA, Lavender H, Gnirss K, Nehlmeier I, Niemeyer D, He Y, Simmons G, Drosten C, Soilleux EJ, Jahn O, Steffen I, Pohlmann S. 2011. Cleavage and activation of the severe acute respiratory syndrome coronavirus spike protein by human airway trypsin-like protease. J Virol 85:13363–13372. https://doi.org/10.1128/JVI.05300-11.
34. Matsuyama S, Ujike M, Morikawa S, Tashiro M, Taguchi F. 2005. Protease-mediated enhancement of severe acute respiratory syndrome coronavirus infection. Proc Natl Acad Sci U S A 102:12543–12547. https://doi.org/10.1073/pnas.0503203102.
35. Kam YW, Okumura Y, Kido H, Ng LF, Bruzzone R, Altmeyer R. 2009. Cleavage of the SARS coronavirus spike glycoprotein by airway proteases enhances virus entry into human bronchial epithelial cells in vitro. PLoS One 4:e7870. https://doi.org/10.1371/journal.pone.0007870.
36. Shirato K, Kawase M, Matsuyama S. 2013. Middle East respiratory syndrome coronavirus infection mediated by the transmembrane serine protease TMPRSS2. J Virol 87:12552–12561. https://doi.org/10.1128/JVI.01890-13.
37. Gierer S, Müller MA, Heurich A, Ritz D, Springstein BL, Karsten CB, Schendzielorz A, Gnirß K, Drosten C, Pöhlmann S. 2015. Inhibition of proprotein convertases abrogates processing of the Middle Eastern respiratory syndrome coronavirus spike protein in infected cells but does not reduce viral infectivity. J Infect Dis 211:889–897. https://doi.org/10.1093/infdis/jiu407.
38. Gierer S, Bertram S, Kaup F, Wrensch F, Heurich A, Krämer-Kühl A, Welsch K, Winkler M, Meyer B, Drosten C, Dittmer U, von Hahn T, Simmons G, Hofmann H, Pöhlmann S. 2013. The spike protein of the emerging betacoronavirus EMC uses a novel coronavirus receptor for entry, can be activated by TMPRSS2, and is targeted by neutralizing antibodies. J Virol 87:5502–5511. https://doi.org/10.1128/JVI.00128-13.
39. Zheng Y, Shang J, Yang Y, Liu C, Wan Y, Geng Q, Wang M, Baric R, Li F. 2018. Lysosomal proteases are a determinant of coronavirus tropism. J Virol 92:e01504-18. https://doi.org/10.1128/JVI.01504-18.
40. Walls AC, Tortorici MA, Snijder J, Xiong X, Bosch BJ, Rey FA, Veesler D. 2017. Tectonic conformational changes of a coronavirus spike glycoprotein promote membrane fusion. Proc Natl Acad Sci U S A 114:11157–11162. https://doi.org/10.1073/pnas.1708727114.
41. Li F, Berardi M, Li WH, Farzan M, Dormitzer PR, Harrison SC. 2006. Conformational states of the severe acute respiratory syndrome coronavirus spike protein ectodomain. J Virol 80:6794–6800. https://doi.org/10.1128/JVI.02744-05.
42. Wang SF, Tseng SP, Yen CH, Yang JY, Tsao CH, Shen CW, Chen KH, Liu FT, Liu WT, Chen YM, Huang JC. 2014. Antibody-dependent SARS coronavirus infection is mediated by antibodies against spike proteins. Biochem Biophys Res Commun 451:208–214. https://doi.org/10.1016/j.bbrc.2014.07.090.
43. Kam YW, Kien F, Roberts A, Cheung YC, Lamirande EW, Vogel L, Chu SL, Tse J, Guarner J, Zaki SR, Subbarao K, Peiris M, Nal B, Altmeyer R. 2007. Antibodies against trimeric S glycoprotein protect hamsters against SARS-CoV challenge despite their capacity to mediate FcγRII-dependent entry into B cells in vitro. Vaccine 25:729–740. https://doi.org/10.1016/j.vaccine.2006.08.011.
44. Jaume M, Yip MS, Cheung CY, Leung HL, Li PH, Kien F, Dutry I, Callendret B, Escriou N, Altmeyer R, Nal B, Daeron M, Bruzzone R, Peiris JS. 2011. Anti-severe acute respiratory syndrome coronavirus spike antibodies trigger infection of human immune cells via a pH- and cysteine protease-independent FcγR pathway. J Virol 85:10582–10597. https://doi.org/10.1128/JVI.00671-11.
45. Corapi WV, Olsen CW, Scott FW. 1992. Monoclonal antibody analysis of neutralization and antibody-dependent enhancement of feline infectious peritonitis virus. J Virol 66:6695–6705.
46. Hohdatsu T, Yamada M, Tominaga R, Makino K, Kida K, Koyama H. 1998. Antibody-dependent enhancement of feline infectious peritonitis virus infection in feline alveolar macrophages and human monocyte cell line U937 by serum of cats experimentally or naturally infected with feline coronavirus. J Vet Med Sci 60:49–55. https://doi.org/10.1292/jvms.60.49.
47. Vennema H, de Groot RJ, Harbour DA, Dalderup M, Gruffydd-Jones T, Horzinek MC, Spaan WJ. 1990. Early death after feline infectious peritonitis virus challenge due to recombinant vaccinia virus immunization. J Virol 64:1407–1409.
48. Du L, Zhao G, Yang Y, Qiu H, Wang L, Kou Z, Tao X, Yu H, Sun S, Tseng CT, Jiang S, Li F, Zhou Y. 2014. A conformation-dependent neutralizing monoclonal antibody specifically targeting receptor-binding domain in Middle East respiratory syndrome coronavirus spike protein. J Virol 88:7045–7053. https://doi.org/10.1128/JVI.00433-14.
49. Du L, Zhao G, Li L, He Y, Zhou Y, Zheng BJ, Jiang S. 2009. Antigenicity and immunogenicity of SARS-CoV S protein receptor-binding domain stably expressed in CHO cells. Biochem Biophys Res Commun 384:486–490. https://doi.org/10.1016/j.bbrc.2009.05.003.
50. He YX, Lu H, Siddiqui P, Zhou YS, Jiang SB. 2005. Receptor-binding domain of severe acute respiratory syndrome coronavirus spike protein contains multiple conformation-dependent epitopes that induce highly potent neutralizing antibodies. J Immunol 174:4908–4915. https://doi.org/10.4049/jimmunol.174.8.4908.
51. Millet JK, Whittaker GR. 2014. Host cell entry of Middle East respiratory syndrome coronavirus after two-step, furin-mediated activation of the spike protein. Proc Natl Acad Sci U S A 111:15214–15219. https://doi.org/10.1073/pnas.1407087111.
52. Walls AC, Xiong X, Park YJ, Tortorici MA, Snijder J, Quispe J, Cameroni E, Gopal R, Dai M, Lanzavecchia A, Zambon M, Rey FA, Corti D, Veesler D. 2019. Unexpected receptor functional mimicry elucidates activation of coronavirus fusion. Cell 176:1026–1039.e1015. https://doi.org/10.1016/j.cell.2018.12.028.
53. Uhlén M, Fagerberg L, Hallström BM, Lindskog C, Oksvold P, Mardinoglu A, Sivertsson Å, Kampf C, Sjöstedt E, Asplund A, Olsson I, Edlund K, Lundberg E, Navani S, Szigyarto CA-K, Odeberg J, Djureinovic D, Takanen JO, Hober S, Alm T, Edqvist P-H, Berling H, Tegel H, Mulder J, Rockberg J, Nilsson P, Schwenk JM, Hamsten M, von Feilitzen K, Forsberg M, Persson L, Johansson F, Zwahlen M, von Heijne G, Nielsen J, Pontén F.

2015. Proteomics. Tissue-based map of the human proteome. Science 347:1260419. https://doi.org/10.1126/science.1260419.
54. Uhlén M, Björling E, Agaton C, Szigyarto CA-K, Amini B, Andersen E, Andersson A-C, Angelidou P, Asplund A, Asplund C, Berglund L, Bergström K, Brumer H, Cerjan D, Ekström M, Elobeid A, Eriksson C, Fagerberg L, Falk R, Fall J, Forsberg M, Björklund MG, Gumbel K, Halimi A, Hallin I, Hamsten C, Hansson M, Hedhammar M, Hercules G, Kampf C, Larsson K, Lindskog M, Lodewyckx W, Lund J, Lundeberg J, Magnusson K, Malm E, Nilsson P, Odling J, Oksvold P, Olsson I, Oster E, Ottosson J, Paavilainen L, Persson A, Rimini R, Rockberg J, Runeson M, Sivertsson A, Sköllermo A, Steen J, Stenvall M, Sterky F, Strömberg S, Sundberg M, Tegel H, Tourle S, Wahlund E, Waldén A, Wan J, Wernérus H, Westberg J, Wester K, Wrethagen U, Xu LL, Hober S, Pontén F. 2005. A human protein atlas for normal and cancer tissues based on antibody proteomics. Mol Cell Proteomics 4:1920–1932. https://doi.org/10.1074/mcp.M500279-MCP200.
55. Qiu H, Sun S, Xiao H, Feng J, Guo Y, Tai W, Wang Y, Du L, Zhao G, Zhou Y. 2016. Single-dose treatment with a humanized neutralizing antibody affords full protection of a human transgenic mouse model from lethal Middle East respiratory syndrome (MERS)-coronavirus infection. Antiviral Res 132:141–148. https://doi.org/10.1016/j.antiviral.2016.06.003.
56. Jing Y, Ni Z, Wu J, Higgins L, Markowski TW, Kaufman DS, Walcheck B. 2015. Identification of an ADAM17 cleavage region in human CD16 (FcgammaRIII) and the engineering of a non-cleavable version of the receptor in NK cells. PLoS One 10:e0121788. https://doi.org/10.1371/journal.pone.0121788.
57. Genin M, Clement F, Fattaccioli A, Raes M, Michiels C. 2015. M1 and M2 macrophages derived from THP-1 cells differentially modulate the response of cancer cells to etoposide. BMC Cancer 15:577. https://doi.org/10.1186/s12885-015-1546-9.
58. Snyder KM, Hullsiek R, Mishra HK, Mendez DC, Li Y, Rogich A, Kaufman DS, Wu J, Walcheck B. 2018. Expression of a recombinant high affinity IgG Fc receptor by engineered NK cells as a docking platform for therapeutic mAbs to target cancer cells. Front Immunol 9:2873. https://doi.org/10.3389/fimmu.2018.02873.
59. Su K, Li X, Edberg JC, Wu J, Ferguson P, Kimberly RP. 2004. A promoter haplotype of the immunoreceptor tyrosine-based inhibitory motif-bearing FcgammaRIIb alters receptor expression and associates with autoimmunity. II. Differential binding of GATA4 and Yin-Yang1 transcription factors and correlated receptor expression and function. J Immunol 172:7192–7199. https://doi.org/10.4049/jimmunol.172.11.7192.
60. Du L, Tai W, Yang Y, Zhao G, Zhu Q, Sun S, Liu C, Tao X, Tseng CK, Perlman S, Jiang S, Zhou Y, Li F. 2016. Introduction of neutralizing immunogenicity index to the rational design of MERS coronavirus subunit vaccines. Nat Commun 7:13473. https://doi.org/10.1038/ncomms13473.
61. Liu C, Tang J, Ma Y, Liang X, Yang Y, Peng G, Qi Q, Jiang S, Li J, Du L, Li F. 2015. Receptor usage and cell entry of porcine epidemic diarrhea coronavirus. J Virol 89:6121–6125. https://doi.org/10.1128/JVI.00430-15.
62. Yang Y, Du L, Liu C, Wang L, Ma C, Tang J, Baric RS, Jiang S, Li F. 2014. Receptor usage and cell entry of bat coronavirus HKU4 provide insight into bat-to-human transmission of MERS coronavirus. Proc Natl Acad Sci U S A 111:12516–12521. https://doi.org/10.1073/pnas.1405889111.
63. Liu C, Ma Y, Yang Y, Zheng Y, Shang J, Zhou Y, Jiang S, Du L, Li J, Li F. 2016. Cell entry of porcine epidemic diarrhea coronavirus is activated by lysosomal proteases. J Biol Chem 291:24779–24786. https://doi.org/10.1074/jbc.M116.740746.
64. Chen Y, Rajashankar KR, Yang Y, Agnihothram SS, Liu C, Lin YL, Baric RS, Li F. 2013. Crystal structure of the receptor-binding domain from newly emerged Middle East respiratory syndrome coronavirus. J Virol 87:10777–10783. https://doi.org/10.1128/JVI.01756-13.